Electronic Supplementary Material (ESI) for Journal of Materials Chemistry A.

Supporting Information

Pressure-Promoted Highly-Ordered Fe-doped-Ni_2B for Effective Oxygen Evolution Reaction and Overall Water Splitting

Ruifeng Tian,†[a] Shijing Zhao,†[b] Junkai Li,†[b] Zhibin Chen,[a] Wenfeng Peng,[b] Yan He,[c] Lili Zhang,[c] Shuai Yan,[c] Lailei Wu,*[a] Rajeev Ahuja,[d] Huiyang Gou*[b]

State Key Laboratory of Metastable Materials Science and Technology, College of Material Science and Engineering, Yanshan University, Qinhuangdao 066004, China. Email: wll@ysu.edu.cn.

Center for High Pressure Science and Technology Advanced Research, Beijing 100094, China. Email: huiyang.gou@hpstar.ac.cn

Shanghai Synchrotron Radiation Facility, Shanghai Advanced Research Institute, Chinese Academy of Sciences, Shanghai 201203, China

Condensed Matter Theory Group, Department of Physics & Astronomy, Uppsala University, 751 20 Uppsala, Sweden

† RT, SZ and JL are contributed equally to this work

Corresponding authors: wll@ysu.edu.cn and huiyang.gou@hpstar.ac.cn

Experimental details

MNiBs synthesis:

Chemicals: iron nanopowder, cobalt nanopowder, nickel nanopowder and amorphous boron nanopowder all bought from Aladdin. All chemicals were used as received without further purification.

Sample preparation: Transition metal powder and boron powder were weighed at mole ratio of mole ratio of 1:1:1.05 for FeNiB and CoNiB and 2:1.05 for Ni_2B and mixed by hand using agate mortar and pestle for no less than 30 min, then pressed into tablets using tabling machine and mold. Samples for HPHT synthesis is assembled with tablets, h-BN and graphite furnace. All steps above were performed under argon atmosphere inside a glovebox to keep oxygen and water free.

HTHP synthesis: two parallel samples for each composition were assembled inside a pyrophyllite cube along with three graphite tablets and two steel caps, then were placed into the cubic press (CS1B, Guilin) chamber. The synthesis is under 5 GPa and 1300 °C for 20 min.

TM_2Bs powder synthesis: TM_2B tablets were cleaned by hand to carve off h-BN on its surface then cleaned with alcohol. The cleaned tables were broken into small pieces with pliers and milled into powder using agate mortar and pestle. The TM_2B powders were further refined with planet ball-milling machine using tungsten carbide pot and balls at 350 rpm for 10h. The refined powders were sealed under argon inside a glovebox to prevent oxidation.

Nickel foam cleaning: In order to remove the protective oil and surface oxidation layer of nickel foam, nickel foam pieces (1cm × 1cm) were cleaned by acetone using an ultrasonic bath for 10 min; then the nickel foam pieces were immersed in 0.5 M HCl for 10 min, finally cleaned with distilled water and ethanol and dried in a drier at 40℃.

Electrode preparation: All three TM_2B samples and commercial RuO_2 were loaded on nickel foam. 4 mg sample along with 1mg carbon black and 30 μ L PTFE (Polytetrafluoroethylene) binder were loaded on a 10 mm × 10 mm bare nickel foam. An Hg/HgO electrode was used as reference electrode and a 10 mm × 10 mm Pt foil electrode as counter electrode. 4mg TM_2B powders and 1mg carbon black were mixed with 30 μl PTFE and 1 ml ethanol and ultrasonic bath for 10 min. The mixture was dried in the drier for 5 min to remove excessive ethanol. Then the mixture was collected and smeared on the cleaned nickel foam using a trace spoon. The smeared surface area covered half surface area of nickel foam, thus the geometry surface area of electrode is 10 mm × 10 mm.

Physicochemical characterization

The crystal structure of synthesized TM_2Bs were examined by X-ray diffraction (XRD) diffractometer (Rigaku D/MAX-2500/PC) with Cu Kα radiation (λ = 1.5406 Å) at 40 kV and 200 mA. The morphology of TM_2Bs were examined by scanning electron microscope (SEM, Hitachi S-4800) and the morphology of FeNiB before and after electrochemical test were examined by

transmission electron microscope (TEM, JEOL JEM-2100F). Their surface elemental compositions and properties were further examined by X-ray photoelectron spectroscopy (XPS, AXIS Ultra DLD, Japan). XAS X-ray absorption spectroscopy (XAS) was performed on the BL15U1 beamline at the Shanghai Synchrotron Radiation Facility (SSRF) and Cornell High Energy Synchrotron Source (CHESS) in United States, and the storage ring was operated at 250 mA mode with a Si (111) double crystal monochromator.

Electrochemical performance test

All electrochemical measurements were carried out in a typical three-electrode setup on a CHI-760e electrochemical workstation. The as-prepared samples were used as working electrodes while a Pt foil and Hg/HgO (1.0 M KOH) electrode served as the counter electrode and the reference electrode, respectively. All tests were conducted in 1 M KOH electrolyte.

The linear sweep voltammetry (LSV) curves were collected at a potential scan rate of 5 mV s^{-1}. All of the measured potentials were converted to the reversible hydrogen electrode (RHE) according to the following equation:

$$E_{RHE} = E_{Hg/HgO} + 0.098 + 0.059pH$$

Electrochemical impedance spectroscopy (EIS) measurements were conducted in the frequency range from 0.1 Hz to 100 kHz at an overpotential of 250 mV (vs. RHE) with a 5 mV sinusoidal perturbation.

The electrochemically active surface area (ECSA) of electrocatalysts was calculated by the following equation:

$$ECSA = C_{dl} / C_s \times S$$

where C_{dl} is determined from cyclic voltammogram (CV) in the double layer region (without faradaic processes) at different scan rates, C_s is a general surface specific capacitance (0.040 $mF \cdot cm^{-2}$ in 1 M KOH for common electrocatalysts) [1], S is the geometric surface area of the electrode (0.5 cm^2 in this work).

The turnover frequency (TOF) of electrocatalysts was calculated by the following equation:

$$TOF = (JA) / (4Fn)$$

Where J is the current density at a certain overpotential, A is the surface area of the electrode, 4 is the mole of electrons transferred to generate one mole of O_2, F is the Faraday constant (96485 $C \cdot mol^{-1}$), n is the number of moles of active sites.

Inductively coupled plasma optical emission spectrometer (ICP-OES)

The ratio of Fe(Co):Ni in FeNiB or CoNiB was also quantitative measured by the inductively coupled plasma optical emission spectrometer (ICP-OES) method (Thermo Fisher, ICAP 6300).

RF power was set at 1150 W. The spectral lines 233.28, 230.79 and 231.60 nm were selected for Fe, Co and Ni respectively. As a result, the obtained atomic ratio of Fe:Ni and Co:Ni were 1:1.03 and 1:1.05 for FeNiB and CoNiB, respectively.

Density functional theory (DFT) calculations

In the present work, we have used the Ab-initio electronic structure calculations based on density functional theory (DFT). A projected augmented wave (PAW) method is used which is implemented in the Vienna ab-initio simulation package (VASP) package. The Perdew-Burke-Ernzerhof (PBE) exchange correlation functional is in the form of generalized gradient approximation (GGA) was used in these calculations. An energy cutoff of 500 eV was used to achieve the energy convergence as well as the force convergence. We used the Brillouin zone (BZ) with a dense Monkhorst-Pack k-grid of 10×10×12 points. The lattice parameters of Ni_2B, Fe_2B and FeNiB single unit cells were optimized prior to electronic properties calculations.

In order to find the most favorable structure of stoichiometric FeNiB, 50% of Ni atoms in Ni_2B structure were replaced by Fe atoms. There are four Ni atoms in Ni_2B primitive cell, thus four different combinations could be made for Fe atom replacement (1-2, 1-3, 1-4, 2-3, 2-4 and 3-4, Figure S1). It turned out that 1-4 and 2-3 were the most stable structure and they are actually the same structure due to the symmetry process. Thus, this structure was adopted for FeNiB electronic calculation.

Tables

Table S1 Results of Rietveld refinements.

	a (Å)	*b* (Å)	*c* (Å)	*a*/*c*	χ^2	R_{wp}	R_p
Ni_2B	4.990	4.990	4.247	1.175	1.82	3.55%	5.95%
CoNiB	5.022	5.022	4.230	1.187	1.66	1.76%	1.2%
FeNiB	5.068	5.068	4.235	1.197	1.98	1.64%	1.17%

Table S2 Summary of bond lengths (in Å) from the Rietveld refinements results.

	B-B	TM-B	TM-TM	TM-TM	TM-TM	TM-TM
Ni_2B	2.123	2.139	2.367	2.420	2.627	2.704
CoNiB	2.115	2.160	2.296	2.460	2.664	2.666
FeNiB	2.118	2.162	2.410	2.420	2.666	2.719

Table S3 The simulation results according to the equivalent circuit model in Fig. 4d. R_{sol}: solution resistance; R_{ct}: charge transfer resistance; R_{oxide}: oxide resistance.

Resistance/Ω	FeNiB	CoNiB	Ni_2B	RuO_2
R_{sol}	2.018	1.672	1.94	1.461
R_{ct}	3.334	43.73	67.94	42.05
R_{oxide}	4.83	21.57	4.68	3.62

Table S4 OER performance of different transition metal boride electrocatalysts.

catalysts	η_{10} (mV)	Tafel slope (mF dec^{-1})	Reference
FeNiB	257.4	110	This work
CoNiB	302.4	120	This work
Ni_2B	300.4	134	This work
Ni_xB/f-MWCNT	286	46.3	[1]
nanocotton-like amorphous Ni-Co-B	300	139	[2]
FeNi@FeNiB-700	272	89.2	[3]
Fe-B-O@FeB_2	260	58.7	[4]
Ni-B-O@Ni_3B	350	80.9	[5]
Fe-Co-2.3Ni-B	274	38	[6]
Boronized NiFe sheet	309	40	[7]
NiCoFeB nanochains	284	46.4	[8]
Co-Ni-B@NF	313	120	[9]
Co-10Ni-B-sp	310	66	[10]
Co-Fe-B-P	225	40	[11]
$Co_2B/CoSe_2$	320	56	[12]

Table S5 Overall water splitting voltage of different electrocatalysts.

Catalysts	Cell voltage@10mA cm^{-2}	Reference
FeNiB	1.538	This work
CoNiB	1.602	This work
Ni_2B	1.621	This work
Ni_xB/f-MWCNT	1.602	[1]
FeNi@FeNiB-700	1.65	[3]
Ni-B-O@Ni_3B	1.58	[5]
Fe-Co-2.3Ni-B	1.52 (@20mA cm^{-2})	[6]
NiCoFeB nanochains	1.75	[8]
Co-Ni-B@NF	1.72	[9]
LiCoBPO	1.53	[13]
Co-Fe oxyphosphide MTs	1.69	[14]
N-$NiMoO_4/NiS_2$	1.6	[15]
Co-Fe-B-P	1.68	[11]
$Co_2B/CoSe_2$	1.73	[12]

Figures

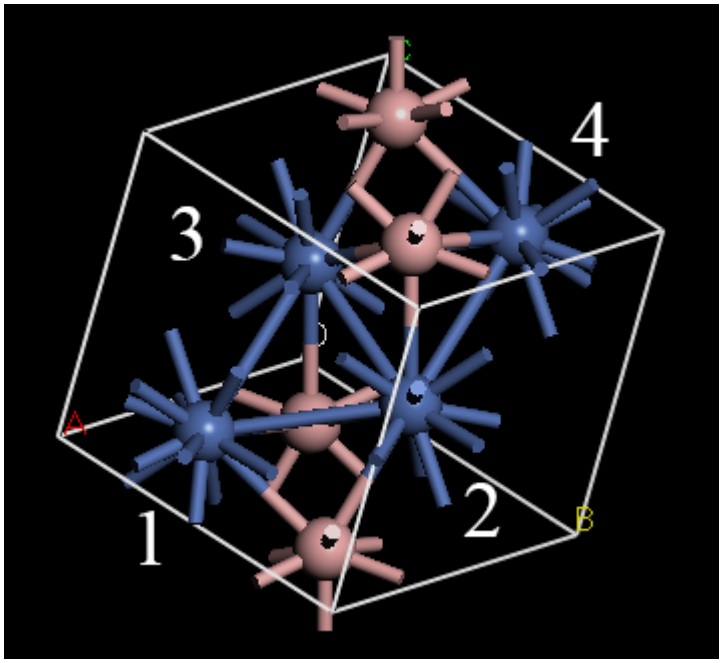

Fig. S1 Illustration of Ni_2B primitive cell and four different atom sites.

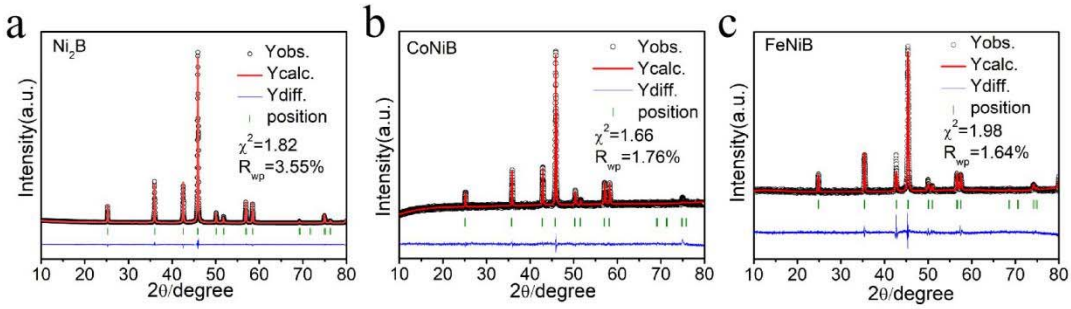

Fig. S2 XRD Rietveld refinement patterns of (a) Ni_2B; (b) CoNiB; (c) FeNiB.

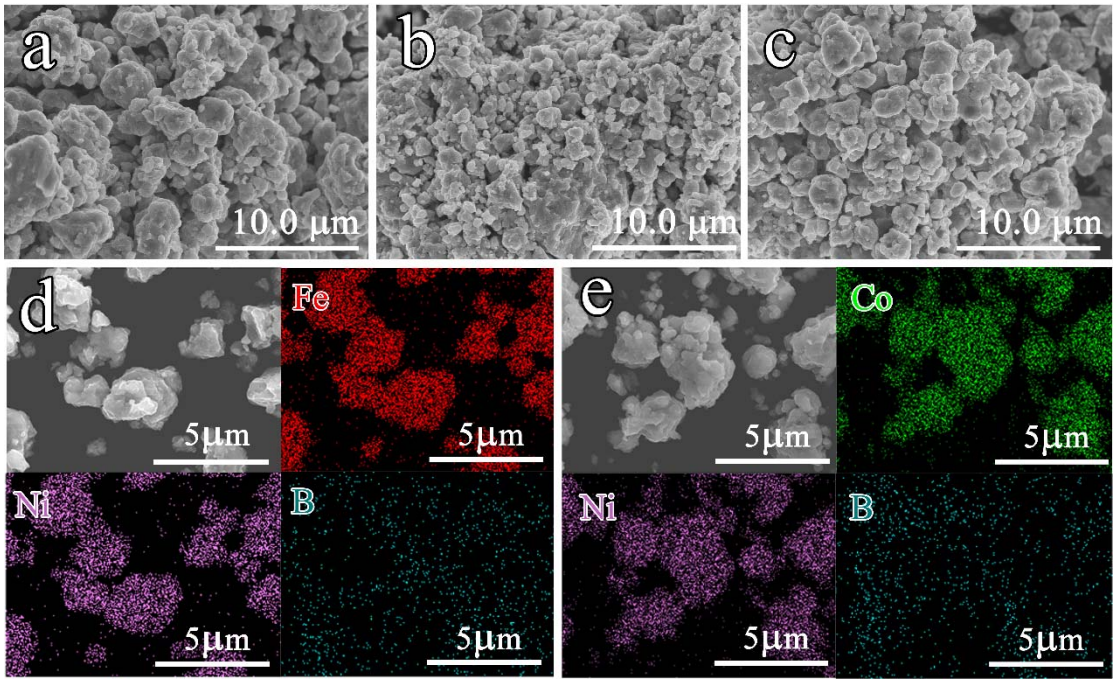

Fig. S3 SEM images of (a) FeNiB, (b) CoNiB and (c) Ni_2B after ball milling for 10h. And EDS mapping results of (d) FeNiB and (f) CoNiB.

a

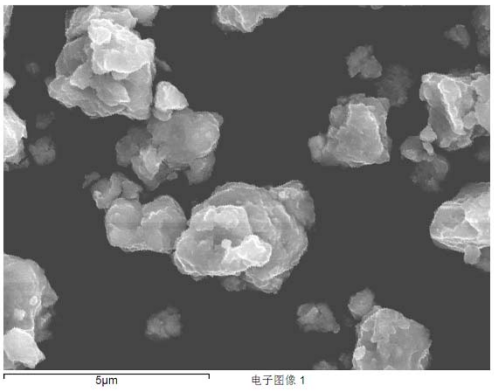

b

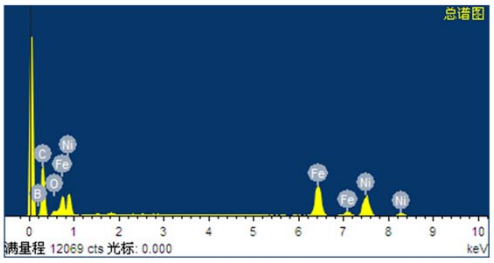

c

FeNiB

Element	wt%	at%
O	6.50	19.94
Fe	44.33	38.96
Ni	49.71	41.40

Fig. S4 EDS mapping results of FeNiB: (a) EDS image; (b) EDS spectrogram; (c) EDS qualification results.

a

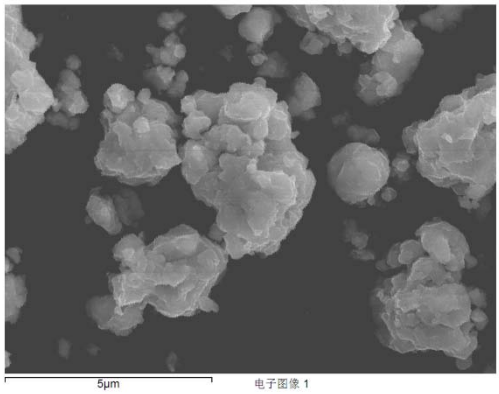

b

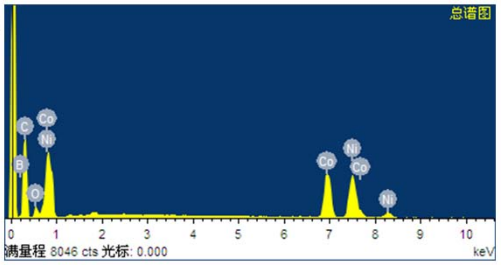

c

CoNiB

Element	wt%	at%
O	5.91	18.76
Co	45.03	38.80
Ni	49.06	42.44

Fig. S5 EDS mapping results of CoNiB: (a) EDS image; (b) EDS spectrogram and (c) EDS qualification results.

a

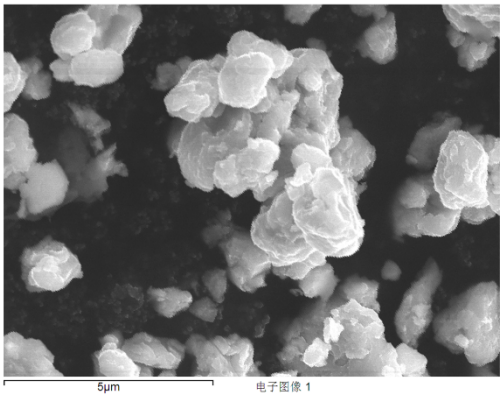

b

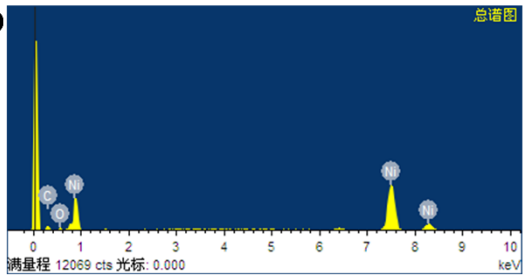

c

Ni_2B

Element	wt%	at%
O	2.50	8.59
Ni	97.50	91.41

Fig. S6 EDS mapping results of Ni_2B: (a) EDS image; (b) EDS spectrogram; (c) EDS qualification results.

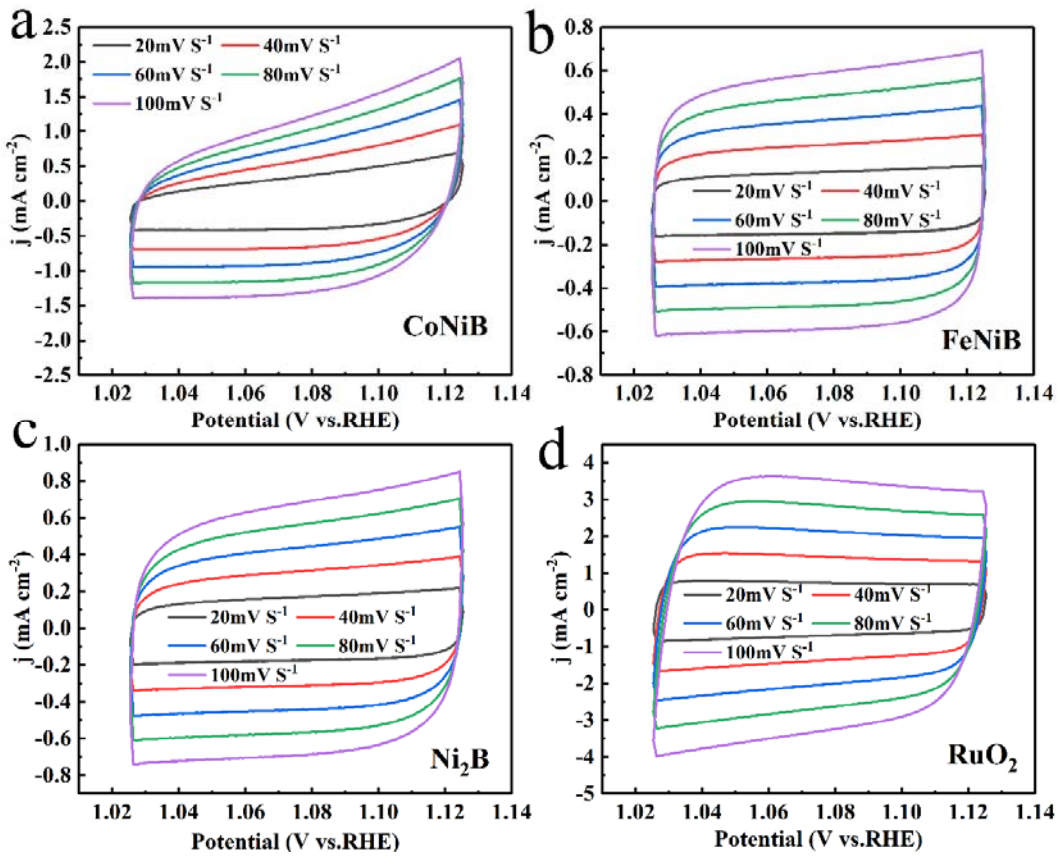

Fig. S7 CV curves for double-layer capacitance measurements under different scan rates from 20 to 100 mV·S^{-1}.

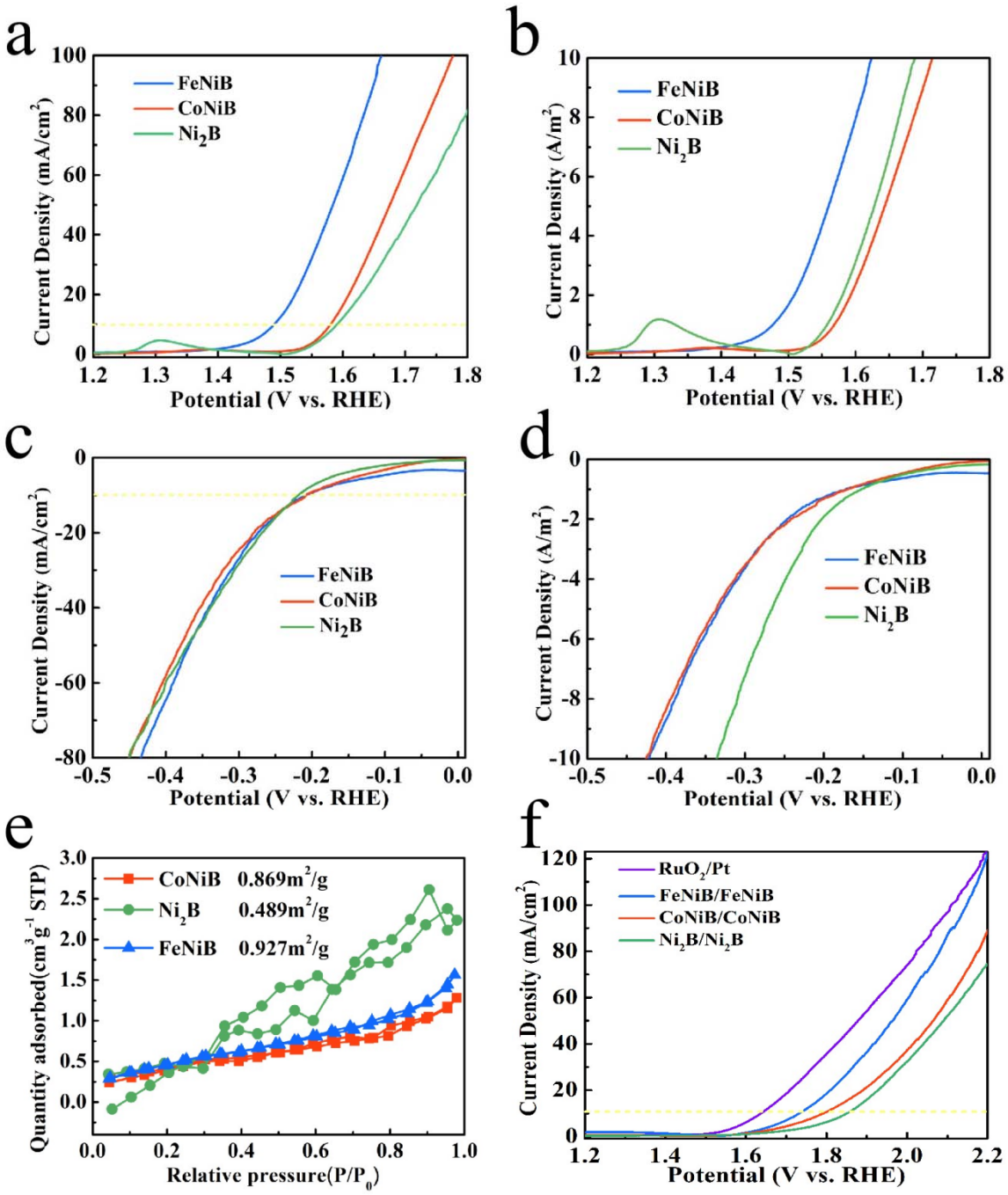

Fig. S8 (a) The OER LSV curves of compounds after several tests. (b) Surface area normalized OER LSV curves in (a). (c) The HER LSV curves of the three compounds. (d) Surface area normalized HER LSV curves.(e) N_2 adsorption-desorption isotherms of the FeNiB, CoNiB, Ni_2B and their specific surface area.(f) The overall water splitting results of different samples.

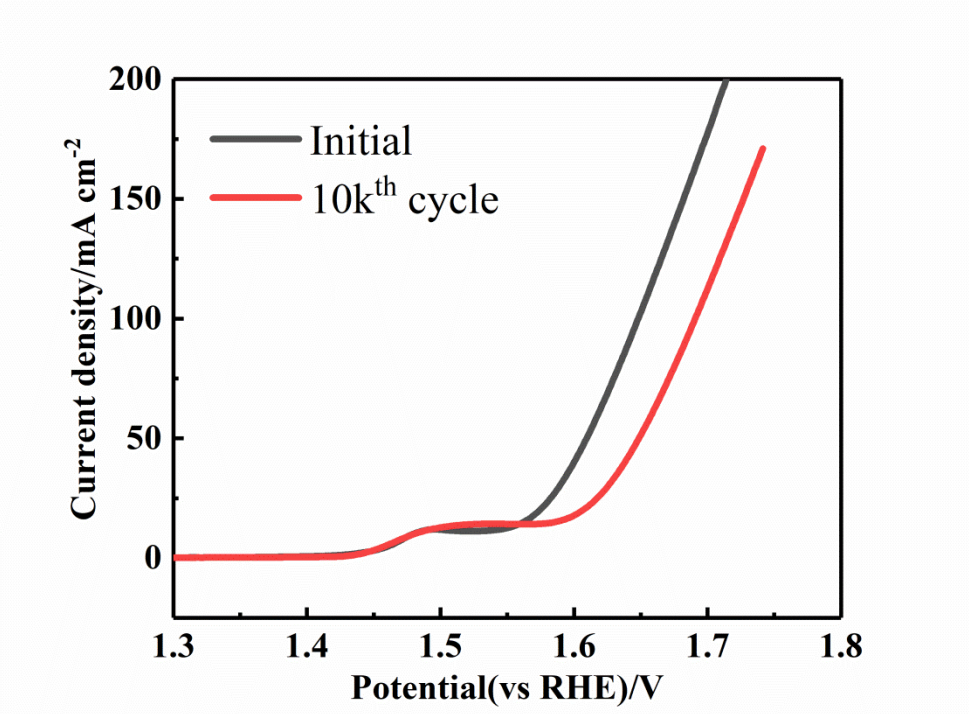

Fig. S9 LSV curve of fresh-made RuO_2 and RuO_2 after cyclic voltammetry for 10k circles.

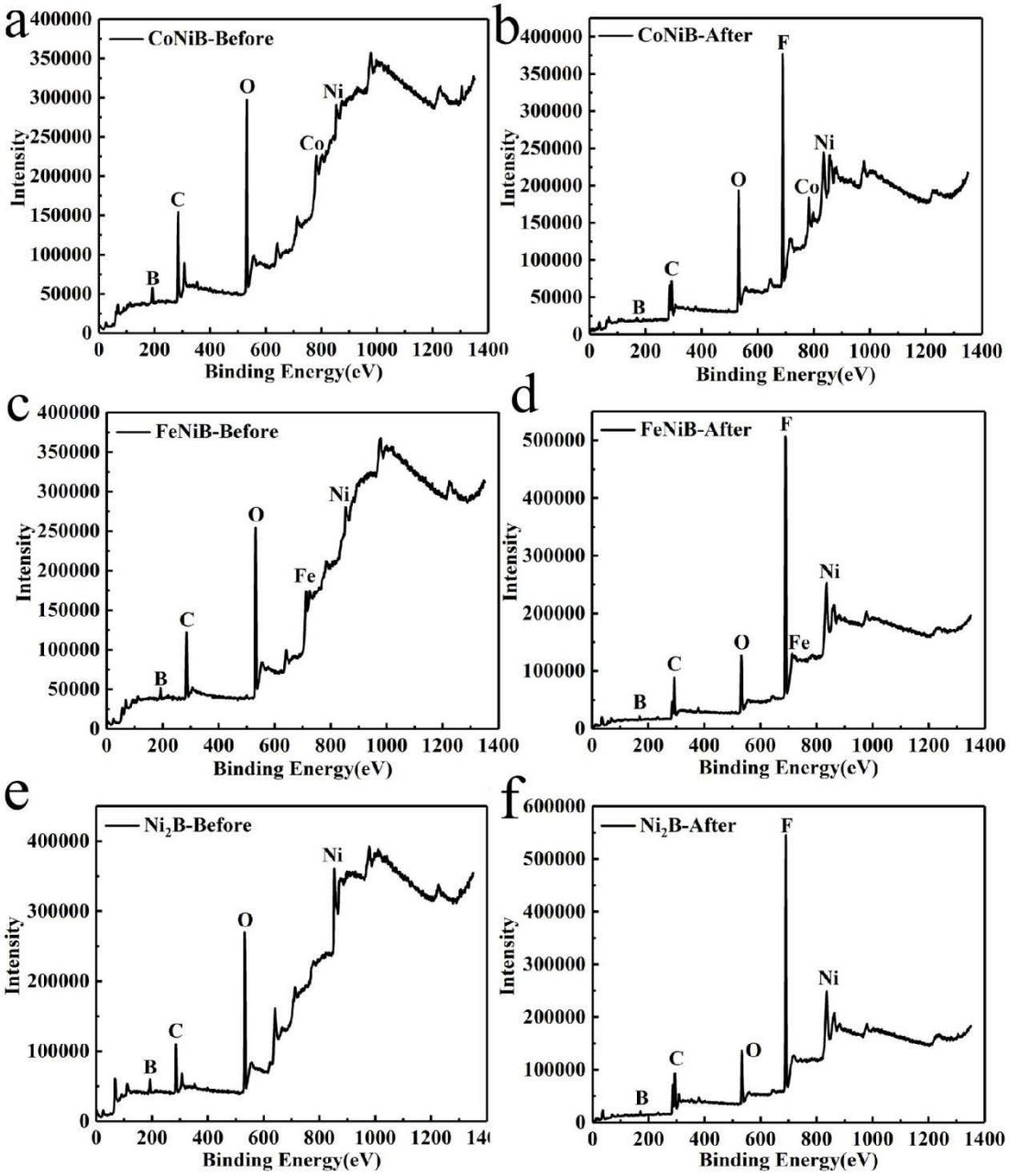

Fig. S10 XPS survey spectrum of CoNiB before (a) and after (b) durability test; XPS survey spectrum of FeNiB before (c) and after (d) durability test; XPS survey spectrum of Ni_2B before (e) and after (f) durability test.

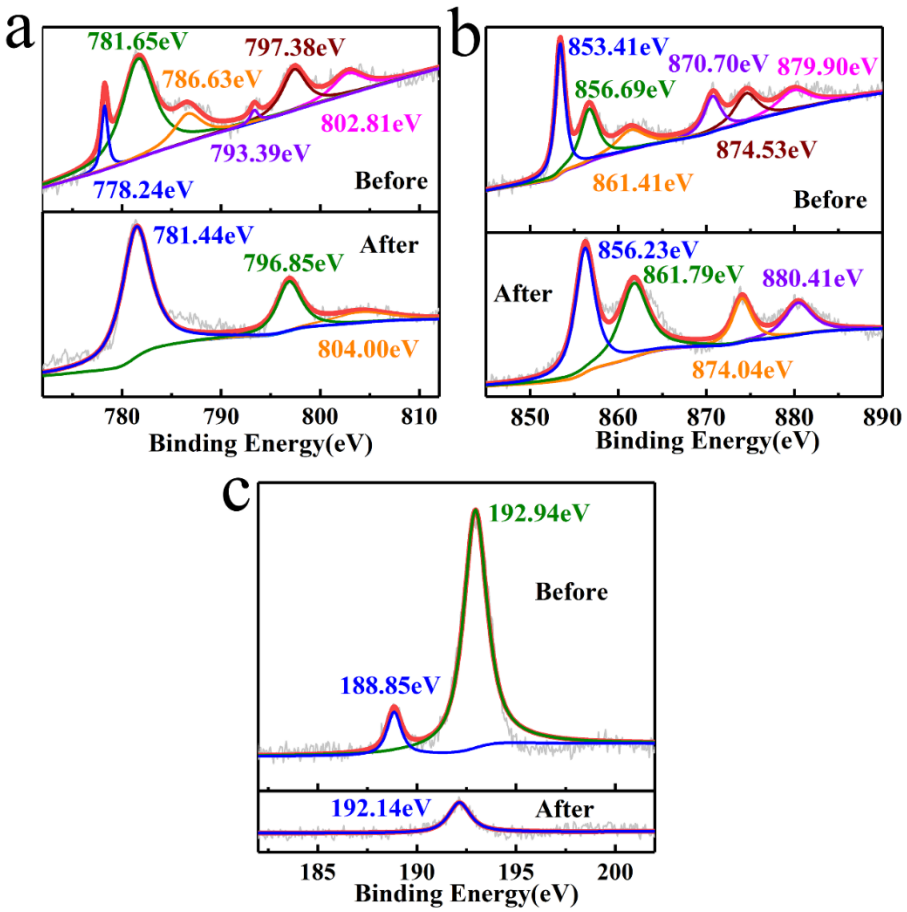

Fig. S11 High resolution XPS spectrum of CoNiB (a) Co 2*p*; (b) Ni 2*p*; (c) B 1s.

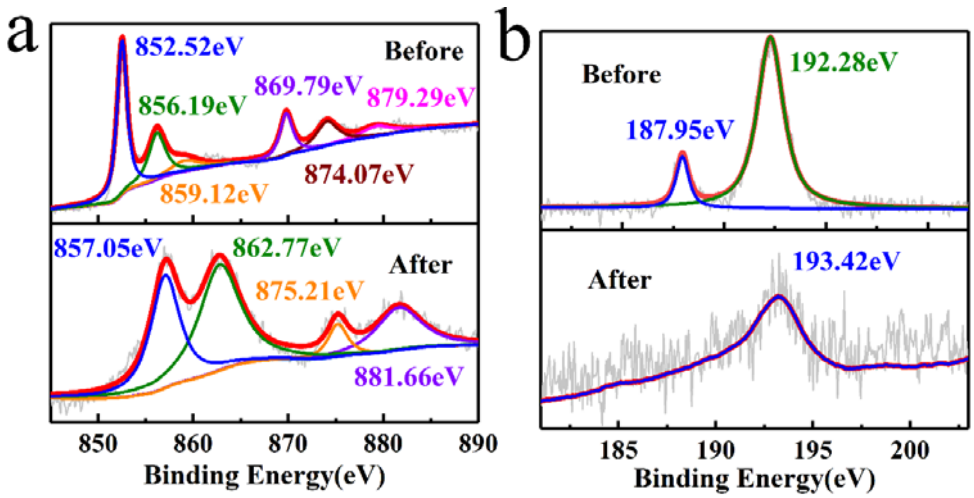

Fig. S12 High resolution XPS spectrum of Ni_2B (a) Ni 2*p*; (b) B 1s.

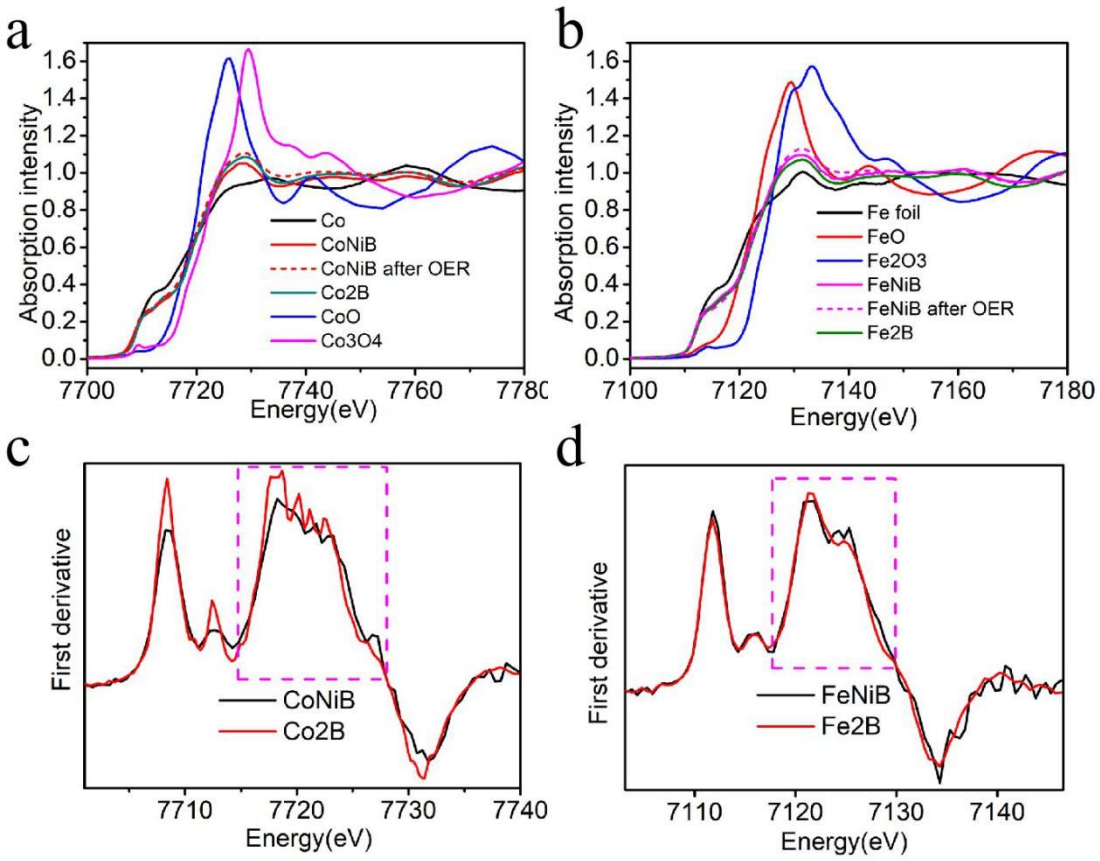

Fig. S13 (a)XANES of CoNiB before/after OER and reference materials collected at Co K edge; (b) XANES of FeNiB before/after OER and reference materials collected at Fe K edge;(c) First derivative of XANES of CoNiB and Co_2B at Co K edge; (d) First derivative of XANES of FeNiB and Fe_2B at Fe K edge.

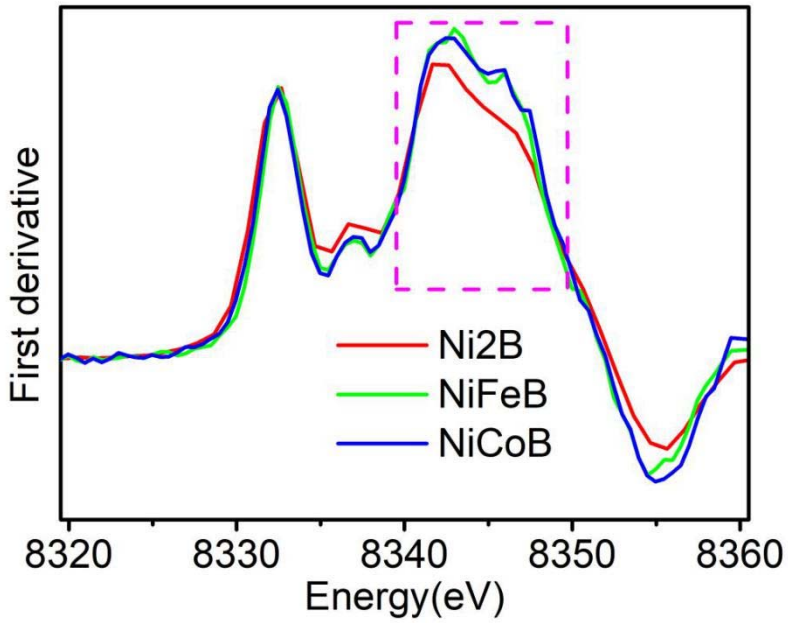

Fig. S14 First derivative of XANES of Ni_2B, NiCoB and NiFeB at Ni K edge.

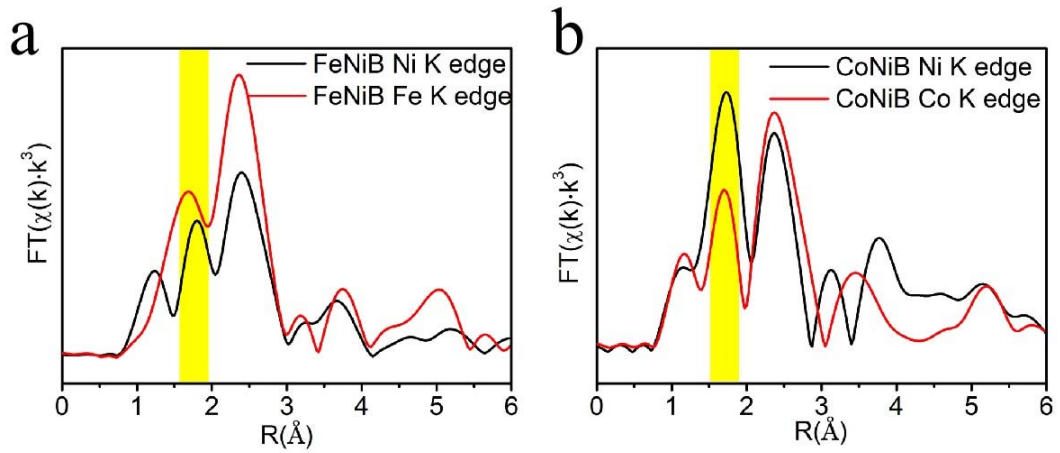

Fig. S15 (a) Fourier transformed k^3 weighted EXAFS oscillations of FeNiB measured at Ni K edge and Fe K edge; (b) Fourier transformed k^3 weighted EXAFS oscillations of NiCoB measured at Ni K edge and Co K edge.

.

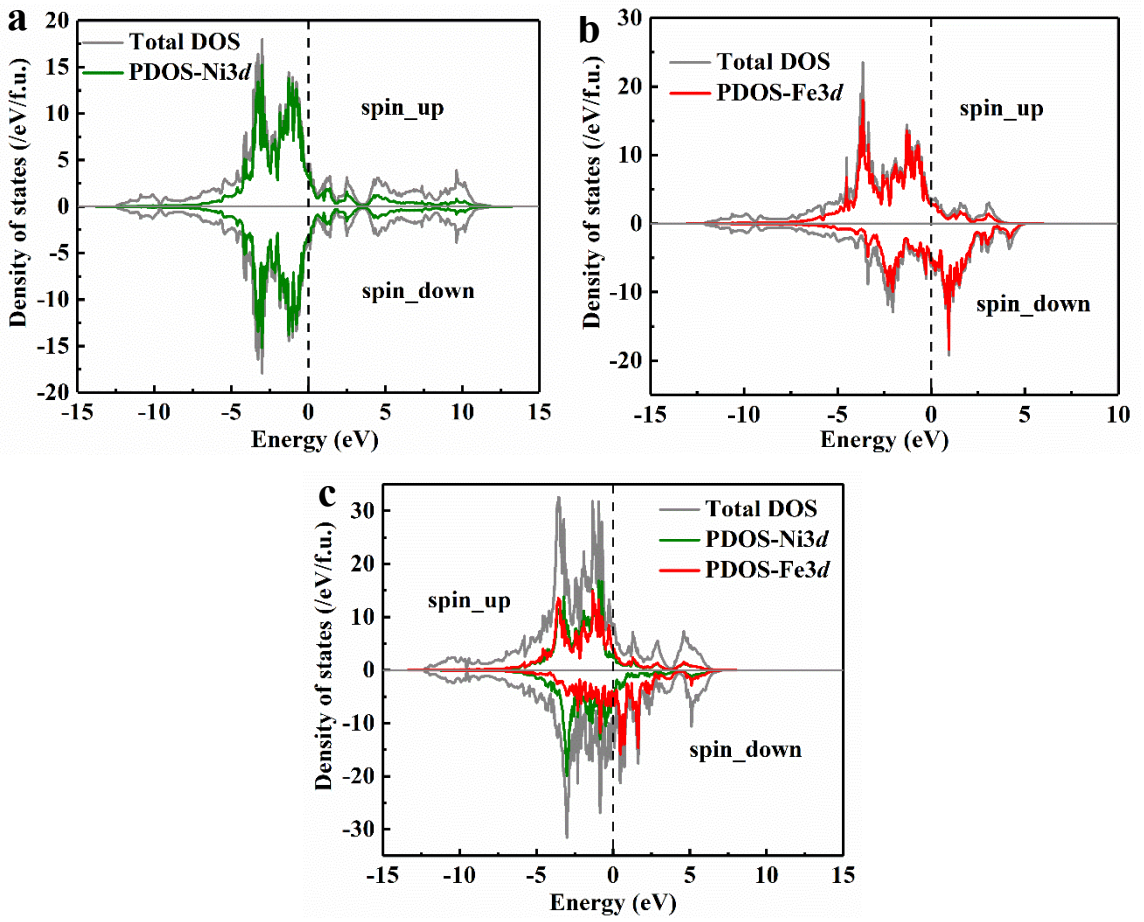

Fig. S16 Total DOS and PDOS of Ni 3d orbital in Ni_2B (a), Fe 3d orbital in Fe_2B (b), Ni 3d and Fe 3d orbital in FeNiB.

Reference

[1] X. Chen, Z. Yu, L. Wei, Z. Zhou, S. Zhai, J. Chen, Y. Wang, Q. Huang, H. E. Karahan, X. Liao, Y. Chen, *J. Mater. Chem. A* 2019, *7*, 764.

[2] S. Wang, P. He, Z. Xie, L. Jia, M. He, X. Zhang, F. Dong, H. Liu, Y. Zhang, C. Li, *Electrochim. Acta* 2019, *296*, 644.

[3] H. Yuan, S. Wang, X. Gu, B. Tang, J. Li, X. Wang, *J. Mater. Chem. A* 2019, *7*, 19554.

[4] L. Wang, J. Li, X. Zhao, W. Hao, X. Ma, S. Li, Y. Guo, *Adv. Mater. Interfaces* 2019, *6*, 1801690.

[5] W. Yuan, X. Zhao, W. Hao, J. Li, L. Wang, X. Ma, Y. Guo, *ChemElectroChem* 2019, *6*, 764.

[6] J. M. V. Nsanzimana, Y. Peng, Y. Y. Xu, L. Thia, C. Wang, B. Y. Xia, X. Wang, *Adv. Energy Mater.* 2018, *8*, 1701475.

[7] F. Guo, Y. Wu, H. Chen, Y. Liu, L. Yang, X. Ai, X. Zou, *Energy Environ. Sci.* 2019, *12*, 684.

[8] Y. Li, B. Huang, Y. Sun, M. Luo, Y. Yang, Y. Qin, L. Wang, C. Li, F. Lv, W. Zhang, S. Guo, *Small* 2019, *15*, 1804212

[9] N. Xu, G. Cao, Z. Chen, Q. Kang, H. Dai, P. Wang, *J. Mater. Chem. A* 2017, *5*, 12379.

[10] J. Zhang, X. Li, Y. Liu, Z. Zeng, X. Cheng, Y. Wang, W. Tu, M. Pan, *Nanoscale* 2018, *10*, 11997.

[11] Z. Wu, D. Nie, M. Song, T. Jiao, G. Fu, X. Liu, *Nanoscale* 2019, *11* 7506.

[12] Y. Guo, Z. Yao, C. Shang, E. Wang, *ACS Appl. Mater. Interfaces* 2017, *9* 3931.

[13] P. W. Menezes, A. Indra, I. Zaharieva, C. Walter, S. Loos, S. Hoffmann, R. Schlögl, H. Dau, M. Driess, *Energy Environ. Sci.* 2019, *12*, 988.

[14] P. Zhang, X. F. Lu, J. Nai, S. Q. Zang, X. W. Lou, *Adv. Sci.* 2019, *6*, 1900576.

[15] L. An, J. Feng, Y. Zhang, R. Wang, H. Liu, G. C. Wang, F. Cheng, P. Xi, *Adv. Funct. Mater.* 2019, *29*, 1805298.